Sulcus detection in planar projections of cortical surfaces

Mutawarra Hussain and Ela Claridge
(M.Hussain, E.Claridge)@cs.bham.ac.uk

School of Computer Science, The University of Birmingham, Birmingham B15 2TT

Abstract. Cortical sulci are important landmarks in neuroimaging. Their localisation and matching in full 3D volumetric images can be complex and compute-intensive. This paper describes a method for finding cortical position of the sulci using quasi-two-dimensional techniques. By applying a hemispherical projection, the cortical part of the brain volume is transformed into a stack of 2D slices, each representing a pixel-deep hemispherical shell. In this representation, cortex forms a nearly-planar surface, while sulci descend into this surface at nearly perpendicular direction. A 3D "slit" filter detects cortical locations of the sulci and generates their 2D map. An application of this map is demonstrated for intra-subject matching of cortical surfaces.

1. Introduction

Cerebral cortex, the outer layer of the human brain, has the form of a thin folded surface. The fold interiors (grooves), called sulci, are important features in studying the brain anatomy and function. The sulci are characteristic of an individual and exhibit pronounced inter-subject variability in location, size and shape. Several sulci (e.g. central and parietooccipital sulcus), which appear quite distinct, are used as landmarks in partitioning the brain into its major functional regions. However, even they are hard to identify in cross-sectional brain images. The automated extraction of sulci from 3D digital image volumes have been studied by a number of groups (e.g. [1], [2]). Because of the complex geometry of the brain and the large volume of data, these methods require substantial computing power.

This paper describes a method for finding the cortical position of the sulci using quasi-two-dimensional techniques which avoid computationally intensive processing of the whole brain volume. Prior to sulcus detection, the brain volume undergoes two geometric transformations. First, the whole volume is mapped into a solid hemisphere through rotation and scaling; the parameters for these transformations are computed from the axes of an ellipsoid fitted to the cortical surface. In the second step, the outer "shells" containing sulci are projected to 2D surfaces using the equal area projection technique [3]. These operations not only reduce the amount of data, but also make the task of extracting sulci as 2D image easy to accomplish.

2. Re-representing volumetric information

Hemispherical projection is a graphical method whereby data on a three-dimensional surface can be represented and analysed in two dimensions. Its main application is mapping of the earth's surface. Whilst mapping a 3D surface onto a 2D plane, it is impossible to preserve exactly both the angular and the area-metric information. The equal area projection has been chosen for this work because of its marginal advantage of having smaller changes near the apex point [3]. The 3D volumetric projection is an extension of the above technique. Instead of the spherical surface, a solid hemisphere comprising of unit-thick shells is given and each shell is mapped onto a 2D plane, 1 unit thick. These 2D planes stacked together form a conical 3D volume. As the radius of the projected area decreases with the decrease of a shell radius, the mapping of a solid hemisphere of radius r results in a cone of height r and base radius $\sqrt{2}r$. Subsequently, the sulci become increasingly oblique near the boundary. Figure 1, left, shows one of the slices in a projected volume. Figure 2, left, shows a cross-sectional view through 53 adjacent slices of the projected volume. A simple scaling factor, a function of the depth of the cone, can transform this cone (excluding the apex point, a projection for $r = 0$) to a cylinder so that the voxels aligned radially in the original projected volume become aligned vertically. Figure 2, right, shows a cross-sectional view through the slices after this transformation. In the resulting volume most of the sulci ascend vertically from the cortical surface. This representation of the cortex, termed the projected volume, contains information about the sulci which is relevant, smaller in magnitude and easier to process, because the sulcus shape is more constrained than in the original volumetric representation.

3. Sulcus extraction

3.1 Problem analysis

A typical projected slice of a T1 weighted MRI volume is shown in Figure 1, left. The sulci appear as dark curves and can be seen clearly in some regions, but less so in others (e.g. near the periphery). Another slice of this projected volume may show sulcus lines clearly near the periphery but have little sulcus information near

the centre. These problems have two main causes: the sulci have different depths; and the brain volume is locally not exactly spherical. Further, although within a slice the tonal relationship between sulci and gyri is consistent (e.g. in T1 images sulci are always darker than gyri), sulcus boundaries are not well defined and their width and length varies. For these reasons, two-dimensional line detection methods applied to individual projected slices fail to reliably detect all the sulci.

However, by considering a cross-sectional view of a stack of projected slices, such as shown in Figure 2, right, the following observations can be made. Sulci extend in depth to many slices. Their depth varies (typical depths observed in this study were 8 to 15 mm), but the width stays relatively constant. Sulci have greater depth than breadth; the opposite is the case for air pockets, whose grey level range is similar to that of sulci. Orientation of sulci w.r.t. the surface varies from vertical (90˚) to oblique (up to 90˚±45˚, typically 90˚±10˚);

These considerations led to the design of a "slit" filter, whose objective is to detect sulci in a projected volume and to record their locations in a 2D image aligned with the topmost projected slice. The ideal filter should not miss a sulcus; it must not respond to features other than sulci; and it should localise sulci accurately. These objectives would be difficult to meet by any single filter that involves no further processing. Rather than searching for an ideal filter in a first instance, the second criterion was relaxed to allow responses to features other than sulci. Any false instances detected by the filter would need to be discarded later on.

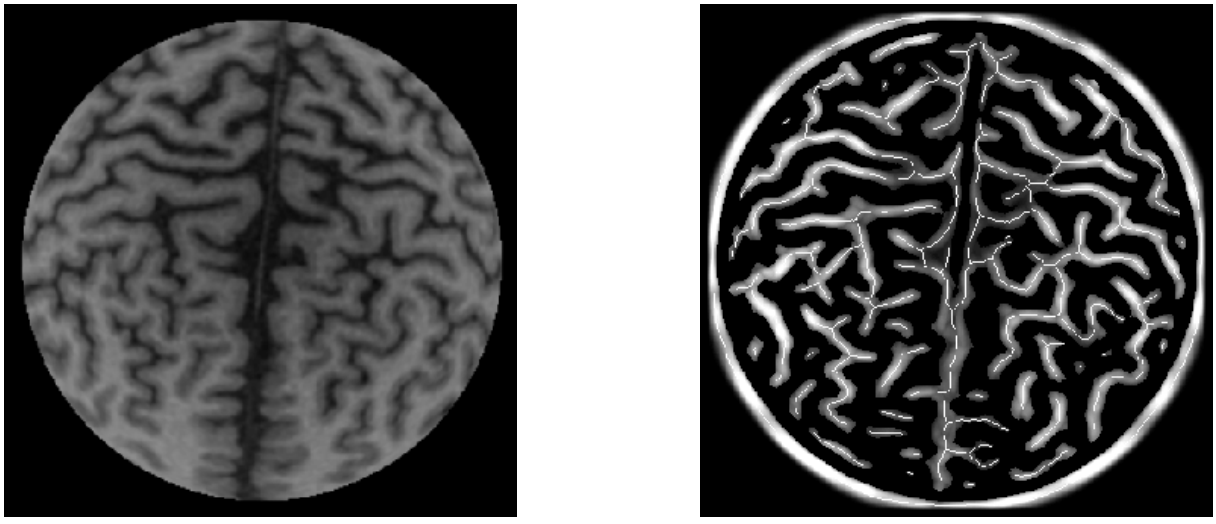

Figure 1. Left: a projected slice of a T1 weighted MRI volume. The sulci appear as dark curves; Right: response of the slit filter (with the lowest responses removed for clarity). The centres of the sulci are shown superimposed in white.

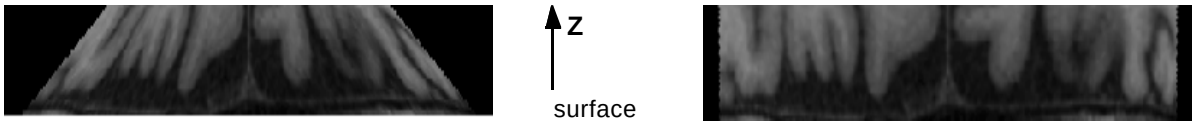

Figure 2. Frontal views of the projected volume: left, the original view; right, the view after angular transformation.

3.2 Development of the slit filter

The slit filter is best thought of as an extension of an oriented line filter, integrated across a number of slices in the projected volume. It's development will be shown here beginning from a 1-dimensional case.

To cater for variability in the sulcus width, a filter based on the difference of offset gaussians (DOOG) [4] was chosen. DOOG consists of a central gaussian lobe $G(\sigma)$, flanked by two gaussian lobes of the opposite sign, $-G(0.5\sigma)$, offset so that the transition zone between the centre and the flanks is (practically) zero. The presence of the "transition zone" makes the filter's response less sensitive to size of the feature than is the case for LOG and DOG filters. Extended to 2D, this filter acquires orientation. The response of an oriented DOOG filter at the 2D image location (x,y) and at orientation θ_i will be denoted $f_{\theta i}(x,y)$. An oriented 2D line filter for a line at angle θ_i is a sum of n DOOG responses in direction orthogonal to θ_i:

$$F_{\theta i}(x,y) = \sum_{n} f_{\theta i}(x^*,y^*) , \qquad (x^*, y^*) \text{ form a line through } (x,y), \text{ orthogonal to } \theta_t \tag{1}$$

Following the principle "the winner takes all", the overall 2D response is taken as the maximum of the directional responses:

$$F(x,y) = \max F_{\theta i}(x,y), \qquad i = 0,...,7 \tag{2}$$

As noted earlier, 2-dimensional features do not reliably identify sulci in single slices. On the other hand, sulci have quite distinct slit-like appearance in a cross-sectioned projection volume. If ϕ_i denotes the angle of the slit w.r.t. z-axis (see Figure 3), the slit filter for ϕ_i is defined as:

$$F^{(\phi i)}(x,y,z) = \sum_z F(x^*,y^*,z) \quad (3)$$

where (x^*, y^*) are the projections of (x,y) on a slice at depth z along angle ϕ_i. Figure 3 shows examples of slit features for $\theta_i = 90^\circ$ and three ϕ_i (0°, -45° and $+45^\circ$). As in (2), the overall 3D response is taken to be the maximum response over ϕ_i:

$$F_{slit}(x,y,z) = \max F^{(\phi i)}(x,y,z),\ -\pi/4 \le \phi_i \le \pi/4. \quad (4)$$

This response is recorded at the entrance to a sulcus in the topmost slice (z=0). Thus the resulting 2D image is a map showing the cortical location of the sulci. This map is thresholded and thinned, resulting in a line map of the sulci.

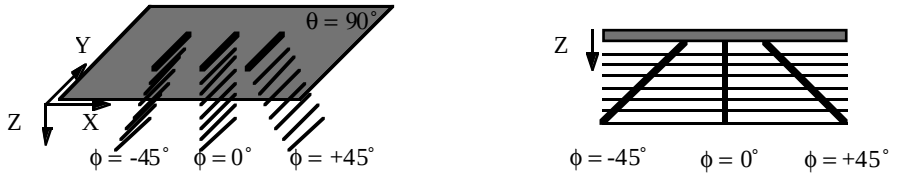

Figure 3. Illustration of 3D slit features. Left: a perspective view; Right: a frontal view with y-axis going into the page. The topmost slice is in grey. Linear features within all the slices have orientation $\theta = 90^\circ$. Angle ϕ between 3D slits and the plane of the topmost slice is -45° for the first slit, 0° for the second and 45° for the third.

Implementation of the slit filter is straightforward and follows the sequence of operations described above. This simplicity is possible, to a large extent, because of the cortex representation as the projected volume constrains sulcus orientations. In all the experiments the same set of parameters was used: $\sigma = 6.0$; $\theta_i = i \cdot \pi/8$, i=0, ...,7; $-\pi/4 \le \phi_i \le \pi/4$.

3.3 Results of the slit filter processing

The performance of the slit filter was evaluated first on simulated data, comprising a volume with slits at different orientations. In the experiments all the slits were detected and the location of slit centres was retrieved with sub-pixel accuracy. Subsequently, the slit filter was applied to a projected MRI volume. In this case only visual analysis was carried out, by superimposing the slit line images over the topmost projected slice. The most striking observation was that there were many false responses, most of which came from pixels belonging to very distinct gyri. The false responses were found to be generated by slit filters oriented perpendicularly to gyri; their magnitude was found to be small. These facts were exploited to eliminate the false responses.

A slit filter designed to give the strongest response to a sulcus, produces a strong *negative* response when applied to a gyrus. A gyrus map, complementary to a sulcus map, can thus be created and the two maps in combination can be used to verify features marked as sulci, as follows. If the magnitude of the response in the sulcus map is significantly greater than in the gyrus map, the sulcus label is confirmed. Otherwise, it is either gyrus (if the gyrus response is much greater) or an undefined feature (both responses are of similar magnitude).

Results of the complete method applied to real data are illustrated on the example of a MRI T1 set of images (256x256x256) of a normal brain. The outer shells containing cortex information were projected to 20 planes. The performance of the filter was assessed visually by superimposing the extracted sulci on the number of slices of the projected volume. The filter successfully differentiated between sulci and other features. The spatial information also appeared quite accurate [5]. Figure 2 shows the sulci extracted from the projected volume (see the slice in figure 1) with the superimposed centre locations of the extracted sulci. It can be seen that the filter responds successfully to the majority of sulci. On the first sight it may appear that there are some incorrect responses. However, when the sulcus lines are placed over further slices (not shown here), it is apparent that there is good overlap over sulci deeper in the volume.

4. The use of sulcus maps

The extracted sulcus maps can be used in several ways. The simplest application is to use them for identification of neuroanatomical landmarks, which are easier to find in a 2D cortical map than in a set of tomographic cross-sections. The identified sulci can then be easily mapped back onto the volumetric representation and used, for example, to relate functional and anatomical aspects of the brain.

Another application, briefly outlined here, is the use of the sulcus maps for matching of cortical surfaces of the same patient, primarily for analysis of temporal changes. A six-stage process is employed as follows. The

two MRI volumes are roughly matched using a rigid-body registration method (e.g. [6]). After mapping to a hemisphere and the hemispherical projection, the sulcus line maps are derived for both image sets, as described above. In the next step, a simple operator detects junctions by identifying pixels with more than two neighbours; this is made easy because the thinning process generates line images exactly 1 pixel thick. Feature space description of the sulcus comprises the spatial position of a junction, the number and orientation of the branches emanating from the junction and, for each branch, the distance to either the next junction or a branch termination point. [7]. Initial matching takes place in the feature space, resulting in the cross-assignment of the junction in the two images. Finally, sulcus registration is refined in the image space, using elastic matching between the sulcus branches [7]. Figures 4 illustrates the results of the matching process.

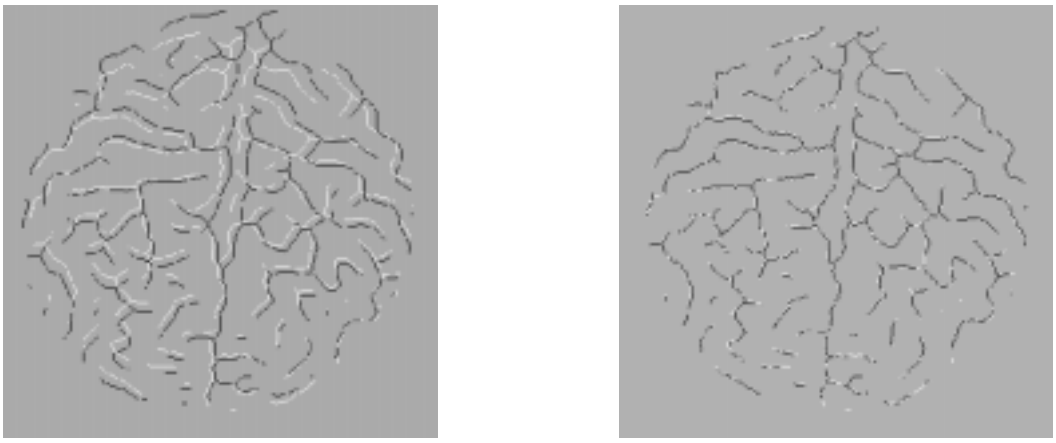

Figure 4. Using the extracted sulci for matching two cortices: left, the sulci extracted from two projected volumes, shown in contrasting colours; right, the aligned sulci on the completion of the matching process.

5. Discussion and further work

The principal objective of this study was to obtain a 2D representation of sulci from a cerebral cortex. The requirements for the technique were that it should be consistent, robust and accurate. Based on a limited number of experiments on real data and on real images, the developed method appears to fulfil these requirements. However, more thorough evaluation is necessary to verify its performance. Further work should also address a number of issues arising from the analysis of the current implementation. Firstly, more accurate localisation of the sulci is possible by replacing a binary thinning process, applied to the thresholded slit filter responses, with the detection of the maximum filter response across the sulcus. This would reduce the localisation error bound which is currently 3mm. Secondly, at present the slit filter shows maxima at locations which correspond to the most prominent in-depth orientation of a sulcus, rather than, as initially envisaged, at the entrance to the sulcus. This, as discussed above, gives an appearance of badly localised sulcus in the top slice of the projected volume. It is necessary to decide which type of response is desirable and to adjust the algorithm accordingly (e.g. by exploiting in-depth connectivity). Future work will also evaluate the clinical value of the sulcus maps in two application areas described in section 4.

References

1. G Lohmann, F Kruggel, DY von Cramon. “Automatic detection of sulcal bottom lines in MR images of the human brain”. *Information Processing in Medical Imaging* (J Duncan, G Gindi Eds), LNCS 1230, pp. 368-374, 1997.
2. G Yaorong et al. “Accurate localisation of cortical convolutions in MR brain images”. *IEEE Trans on Medical Imaging*, 15(4), pp.418-428, 1996.
3. JE Jackson. *Sphere, Spheroid and Projections for Surveyors*. Granada Publishing, 1980.
4. RA Young. “The Gaussian derivative model for machine vision: visual cortex simulation”. *Technical Report GMR-5323, General Motors Research Laboratories*, 1986.
5. M Hussain. Image registration: extraction of sulci using the hemispherical projection technique. *Technical Report CSR-99-4*, School of Computer Science, The University of Birmingham, 1999.
6. M Hussain. Intra-modality image registration using gradients. *Technical Report CSR-98-12*, School of Computer Science, The University of Birmingham, 1998.
7. M Hussain. Image registration: matching the sulci. *Technical Report CSR-99-5*, School of Computer Science, The University of Birmingham, 1999.